High-rate activated sludge at very short SRT: Key factors for process stability and performance of COD fractions removal

Joan Canals [a,b], Alba Cabrera-Codony [a], Oriol Carbó [a,b], Josefina Torán [b], Maria Martín [a], Mercè Baldi [b], Belén Gutiérrez [b], Manel Poch [a], Antonio Ordóñez [b], Hèctor Monclús [a,*]

[a] *LEQUIA, Institute of the Environment, Universitat de Girona, c/Maria Aur..lia Capmany i Farn..s, 69, Girona 17003, Catalonia, Spain*
[b] *GS Inima Environment, S.A. c/Gobelas 41. 1ª A, Madrid 28023, Spain*

ABSTRACT

In high-rate activated sludge (HRAS) processes, reducing the solid retention time (SRT) minimizes COD oxidation and allows to obtain the maximum energy recovery. The aim of this research was to operate a pilot plant with an automatic control strategy to assure the HRAS process stability and high COD fractions removal at very low SRT. This study combines simulation and experimental tools (pilot plant 35 $m^3 \cdot d^{-1}$) operating at SRT (0.2 d), HRT (0.6 h) and DO (0.5 mg$\cdot L^{-1}$) treating high-strength raw wastewater, at 18–26°C, at variable flow. The research includes the effects of temperature, influent concentration and MLSS reactor concentration over the sCOD, cCOD and pCOD removal.

The study points out that the best parameter to control the HRAS at a low SRT is not strictly the SRT but rather the reactor MLSS concentration: operating at 2,000±200mg$\cdot L^{-1}$ assured a stable process despite the large influents variation. Low SVI values of 50–70ml$\cdot g^{-1}$ indicated the good settling properties of the biomass. With only a 6.9% COD oxidation, a high organic matter removal (57±9% for COD and 56±10% for BOD$_5$), was reached. The high removal efficiencies for pCOD (74%) compared to the (29%) for sCOD and (12%) for cCOD also confirmed the importance of settling efficiency and stability in the HRAS. The direct correlation between COD influent and COD removal makes advisable to use the HRAS as a replacement of the primary clarifier. The HRAS acted efficiently as a filter for COD and pCOD peak loads and, in a lesser extent, for BOD$_5$, while sCOD peaks were not buffered. The adopted model presented a good fit for COD fractions except for pCOD when the temperature exceeds 23 °C.

1. Introduction

The conventional activated sludge (CAS) process has proven its efficacy and adaptability in meeting new effluent quality standards for wastewater for more than a century. However, it is a high-energy consuming process with a significant environmental impact. As a result, there has been a significant increase in the development of more sustainable technologies aimed at reducing energy consumption and environmental impacts. Only approximately (35–40%) of the influent organic matter,measured as COD, is removed by primary clarifier (PC) (Crites and Tchobanoglous, 1998) and sent to anaerobic digestion for energetic valorisation as biogas; the remaining 60%−65% goes directly to CAS, with its corresponding oxygen consumption (Seeley, 1992). Improving the effectiveness of the PC is therefore crucial to reduce the overall electricity consumption (Huang and Li, 2000; Li, 1998; Ross and

Crawford, 1985; Yetis and Tarlan, 2002). Municipal wastewater with 500 mg$\cdot L^{-1}$ of COD contains around 1.9 kWh$\cdot m^{-3}$ of energy stored in the chemical bonds (Mccarty et al., 2011), while the energy required in conventional wastewater treatment plants (WWTPs) is in the range of 0.3–0.7 kWh$\cdot m^{-3}$ (Jimenez et al., 2015). Therefore, there is a great potential for improving the energy recovery in WWTPs and several studies proposed to enhance the PC efficiency in order to derivate more COD to anaerobic digestion and reduce the organic load to the following conventional activated sludge. Different alternatives have been suggested: Dynamic sand filtration, dissolved air flotation, chemical enhanced primary treatment, and high-rate activated sludge (HRAS) process (Sancho et al., 2019).

The HRAS process enhances the removal of particulate and colloidal COD (pCOD, cCOD), and even some of the soluble COD (sCOD), with a minimum energy consumption (Christian et al., 2008; Constantine et al.,

---

2012; Jimenez et al., 2015; Nogaj et al., 2015; Rahman et al., 2019; Wett et al., 2007; Yeshi et al., 2014). HRAS removes the wastewater organic load using two different mechanisms:

1) Carbon redirection, where particulate and colloidal fractions are removed by bioadsorption (bioflocculation) and redirected into the sludge matrix, while soluble biodegradable COD is removed by intercellular storage (bioaccumulation), microbial growth and carbon oxidation. The bioadsorption capacity is usually affected by the size of the organic compounds, the shear rate, the presence of available sorption sites on the sludge, the characteristics of the mixed liquor and the organic loading rate (OLR) (Modin et al., 2016).

2) Carbon harvesting, where redirected organic carbon is recovered through settling without having been metabolized by bacteria and sent to anaerobic digestion (Modin et al., 2016; Rahman et al., 2016; Rosso, 2019). One factor that limits carbon harvesting is the settling capability of the biological sludge. Meerburg (2016) compared the SVI of biological sludge at 1 hour and 8.45 h HRT (achieving SVI values of 76 and 120 ml·g^{-1}, respectively) and concluded that the lower the HRT was, the higher the settleability of biological sludge. Similar conclusions were drawn by Miller (2015) and Rahman et al. (2019). However, Jimenez et al. (2015) and (Rosso, 2019) found that the low oxidation of organic matter due to the low SRT maximizes the organic matter redirection but decreases the settling of biomass and consequently worsens the harvesting.

Different HRAS configuration have been developed, such as A-Stage and High-Rate-CS (Carrera et al., 2022; Rahman et al., 2019). Rahman et al. (2017) proposed the use of the High-Rate-CS process for influents with low organic matter concentrations, such as those from a chemically enhanced primary treatment (CEPT) process, while the use of the A-Stage process was proposed for effluents with high organic concentrations, such as raw wastewater. Tirkey et al. (2022) studied an anoxic HRAS for nitrogen (denitrification) and carbon recovery, and Wett et al. (2020) the HRAS Sequencing Batch Reactor with high thickening capabilities.

HRAS process operates at low hydraulic retention time (HRT), usually below one hour, and at low solid retention time. However, when the HRAS treats the primary settler's effluent it operates at longer HRT since the percentage of particulate and colloidal fractions are lower, thus the HRAS depends on the wastewater conditions (Carrera et al., 2022; Rey-Martínez et al., 2021; Zhang et al., 2021). Likewise, HRAS working at short HRT presents lower influent flow dilution compared to CAS processes (HRT of 6–9 h) resulting in a limited buffering capacity of the influent changes (Miller et al., 2017). This is not in contradiction with the fact that the HRAS process reduces the fluctuations of the subsequent nutrient elimination process.

Thus, HRT must be long enough to allow the biomass development and the biosorption process, while short enough to limit the COD mineralization. Likewise, the SRT must be set to optimize the sludge concentration, the biomass yield and the efficiency of the system (Sancho et al., 2019). Previous studies working with raw wastewater reported the impact of SRT, HRT and DO on the HRAS performance: Jimenez et al. (2015) in a HRAS laboratory pilot plant at 0.3 d SRT and 20–25 °C, indicated that SRT, HRT and DO had a high impact on cCOD and pCOD removal efficiency, but lower impact on sCOD removal. Rahman et al. (2016) in laboratory pilot plants working at 0.3 d SRT, 20 °C, observed that HRAS had higher pCOD (74%) and COD (67%) removal efficiency than High-Rate-CS, pCOD (55%) and COD(54%) but similar for sCOD (56–50%) and cCOD (35–25%). Miller et al. (2017), in a HRAS pilot plant at 0.1–0.3 d SRT, 15–25 °C evaluated the use of oxygen DO and MLSS concentration to control the process.

There is an optimal SRT where carbon capture is maximized (0.25–0.4 days), while below ca. 0.2 days less COD is oxidized and only a small fraction is removed from the wastewater. SRT over 1 day leads to an increase of COD hydrolysis and oxidization, including a fraction of primary solids (Jia et al., 2020; Miller, 2015). Haider et al. (2003) found that working at a SRT shorter than one day produced a selection of fast-growing bacteria: A-Stage Heterotrophic Organisms (AHO) that use the sCOD only partially, in accordance with Böhnke et al. (1997) who observed that HRAS systems only supported AHO, while CAS systems had a rich community of bacteria, protozoa and metazoans. Hauduc et al. (Hauduc et al., 2019) indicated that at SRTs lower than 3 days, AHOs are preferably developed, avoiding cell lysis and endogenous respiration and consequently minimizing oxygen consumption. Due to the short SRT, the HRAS process retains only the AHO that can only use rapidly degradable substrates, for instance, volatile fatty acids (VFA) and monomers. They also proposed a model that includes a readily biodegradable substrate, S_B, split into $S_{B,mono}$ and $S_{B,poly}$. In addition, the flocculation of suspended solids and colloids, which correlates closely with the total biomass concentration, is affected by the temperature and mixing intensity, represented in the model by a flocculation factor. A deflocculation process in the recirculation pumping is also considered.

In the past years, modelling tools for HRAS process have been shown to be critical for improving system performance and designing new systems. Haider et al. (Haider et al., 2003) in HRAS modelling studies, also proposed additional fractioning of sCOD to justify its incomplete degradation by AHO in the HRAS process. Their model described the removal of sCOD omitting COD adsorption. Later, Nogaj et al. (2015) and Takács Takács (2021) developed a model to describe the organic substrate transformation in the HRAS process, which included: dual soluble substrate utilization; production of extracellular polymeric substances (EPS); absorption of soluble substrate (storage); and adsorption of colloidal substrate.

Until now, many HRAS pilot plant studies have been basically focussed on describing the impact of SRT, HRT and DO on the HRAS performance. However, process stability is poorly understood. As a novelty, this paper addresses the research to ensure a proper stability of the HRAS process, operating an HRAS pilot plant at extreme conditions (SRT < 0.5 d HRT < 1 h and DO < 0.5 mg·L^{-1}). Moreover, the use of real high-strength wastewater at variable flow without temperature correction, with a previous anoxic zone and two alternative clarifiers, is a significant difference with previous studies. Furthermore, the process performance was validated through the process simulation, a comparison that usually lacks in this kind of studies.

Thus, the main objective of this study was to evaluate the stability of the HRAS process at such operating conditions by: i) Maintaining MLSS concentration at 2000 mg·L^{-1} as control strategy; ii) Evaluating the removal efficiency of each COD fraction and BOD_5 and their correlations with key operational process parameters; iii) Monitoring the influent and effluent COD fractions and BOD_5 in long-term operation; iv) Evaluating the COD oxidation; v) Comparing the simulated COD fractions removal efficiency with the pilot plant results.

2. Materials and methods

2.1. Pilot plant description

A pilot plant was designed to perform this research following the scheme presented in Fig. 1. It was operated with pre-treated wastewater (grit and scum removal) from the WWTP of the municipality of Montornès del Vallès (Barcelona, NE Spain) serving a population of 95,000 eq. inhabitants with significant load variations due to the industrial activity (30–40%). A screen system with a 5 mm mesh was installed to remove tlarge solids from the influent.

Different operation periods were designed, where the flow rate was set constant or variable to mimic a real WWTP. The average daily flow range between 24.1–31.8 m^3·day^{-1}. The plant was composed by two 0.8 m^3 biological reactors (R1 and R2) with 2 m^3·h^{-1} recirculation pump and 0.5 m^3·h^{-1} wasting pump. The reactor R1 was installed previous to the aerobic reactor R2 to analyse the effect of flocculation over cCOD and pCOD removal.
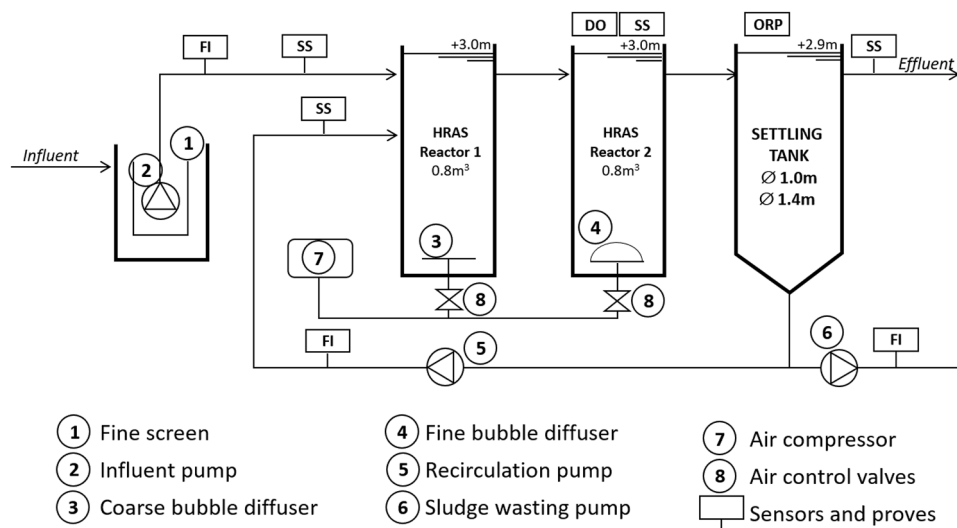
Fig. 1. Pilot Plant Process Diagram.

The pilot plant was provided with two clarifiers (1.0 and 1.4 m diameter) that were operated alternatively and allowed to modify the OFR and SL without changing the HRT of the reactor, which constituted a singularity of the present study. The side water depth in the reactors and settling tanks was 3.0 m. Aeration in Reactor R2 was controlled using a DO sensor (Hach Lange) and a motorized valve with automatic PID control. The air supplied in reactor R1 was only to prevent the accumulation of MLSS at the bottom of the reactor, the overflow rate was 7.14 m·h^{-1}, enough to keep the biomass in suspension.

2.2. Sampling and analysis

The plant was equipped with two automatic samplers to collect and keep refrigerated at 5°C 24-hour, influent and effluent integrated samples (Hach Lange). The analysis included COD (soluble, colloidal, and particulate), BOD$_5$, TSS, VSS, N-TKN, N-NH$_4^+$, TP and P-PO$_4^{3-}$ according to standard methods [26]. There were 92 days of representative results of the process. Days with extreme incidents in the influent were disregarded.

The COD fractions (particulate, soluble and colloidal) were calculated as follows: pCOD difference between total COD and filtered COD through 1,5 μm; sCOD flocculated (ZnSO4) and filtered through 0.45 μm (Mamais et al., 1993); cCOD difference between pCOD and sCOD . The BOD$_5$ analysis was performed with seed inoculum from a CAS plant, not from the HRAS reactor.

Solid samples were collected twice a week from the reactors and recirculation and were analysed for TSS, VSS and COD, always following the recommendations prescribed in the standard methods ((APHA), 2005).

The pilot plant continuously monitored the following operational parameters: DO (reactor 2), ORP (bottom of clarifier), influent flow rate, recirculation flow rate and waste flow rate. The suspended solids in the influent, reactor R2, effluent and recirculation flow were continuously analysed by means of four digital sensors (Solitax sensor, Hach). Due to biofouling in the reactor, the DO sensor was equipped with an air blast-cleaning mechanism. The ORP sensor was installed in order to avoid anaerobic conditions in the bottom of clarifier.

2.3. Pilot plant influent wastewater characteristics

Table 1 summarizes the average characteristics of the influent, including raw wastewater and internal WWTP recirculation. It can be observed that COD was composed by a soluble fraction of 25% and particulate and colloidal fractions of 75%. This large proportion of non-

Table 1
Pilot plant influent characteristics.

Parameter	Acronym	Average ± S.D.	Units
Chemical Oxygen Demand	COD$_{IN}$	686 ± 212	mg·L^{-1}
Particulate Chemical Oxygen Demand	pCOD$_{IN}$	456 ± 201	mg·L^{-1}
Colloidal Chemical Oxygen Demand	cCOD$_{IN}$	62 ± 24	mg·L^{-1}
Soluble Chemical Oxygen Demand	sCOD$_{IN}$	171 ± 60	mg·L^{-1}
Biochemical Oxygen Demand	BOD$_{5IN}$	254 ± 109	mg·L^{-1}
Total Suspended Solids	TSS$_{IN}$	399 ± 175	mg·L^{-1}
Volatile Suspended Solids	VSS$_{IN}$	297 ± 156	mg·L^{-1}
Total Kjeldahl Nitrogen	N-TKN$_{IN}$	70 ± 15	mg·L^{-1}
Ammonium Nitrogen	N-NH$_{4IN}^+$	38 ± 9	mg·L^{-1}
Total Phosphorous	TP$_{IN}$	8.7 ± 3.4	mg·L^{-1}
Orthophosphates	P-PO$_{4IN}^{3-}$	1.7 ± 0.8	mg·L^{-1}
Reactor Temperature (*range*)	T	1 8–26	°C

soluble COD makes that the main potential for energy recovery and savings relies on the capture of colloidal and particulate fractions and limiting the oxidation of the soluble fraction.

The sewage collection system was by gravity, which meant that non-septic water conditions were present in the influent. The standard deviation (SD) of the averaged parameters is high as usual in a municipal wastewater with high industrial loadings.

2.4. Pilot plant operating conditions

The pilot plant was operated during 497 days, running over nine different operational periods, the main parameters and conditions of which are summarized in Table 2 and Table 3. Aside from the inherent variations in the influent water characteristics, the differences of operational parameters during the different periods were the flow rate: constant (CF) or variable (VF) according to the schedule in Table S1; the point of sludge wasting: from the reactor (R2) or from the clarifier (STL) and the settler diameter: 1.0 o 1.4 m. The HRT on the reactor R2 was 0.6 h (Periods 1–9), while R1 was operated at HRT 0.6–0.8 h during periods 1–6. The SRT was maintained under 0.5 days.

The SRT (0.2 ± 0.05 days) was maintained practically constant in the low range during the whole operation to minimize sCOD oxidation. The SRT calculations (Eq. S1, Supplementary information) omitted the biomass in the clarifier, the suspended solids in the influent and the suspended solids in the anoxic reactor. Hydraulic retention time (HRT) was calculated (Eq. S2), without considering the recirculation flow.

Solids Loading (SL) is the ratio between the amount of mixed liquor suspended solids (MLSS) coming into the settler and the settler surface

Table 2

Pilot plant operating conditions in each experimental period.

Period [days]	Inflow [m³·d⁻¹]	Inflow regime	Wasting point	Reactors in operation	Temperature R2 [°C]	Clarifier Diameter [m]
1 (86d)	24.1	CF	R2	R1 + R2	18.5	1
2 (44d)	29.3	CF	STL	R1 + R2	22.1	1
3 (80d)	31.8	CF	STL	R1 + R2	25.6	1
4 (58d)	30.8	VF	STL	R1 + R2	26.3	1
5 (37d)	30.7	VF	STL	R1 + R2	22.8	1
6 (31d)	31.1	VF	STL	R1 + R2	19.3	1.4
7 (41d)	31.1	VF	STL	R2	18.9	1.4
8 (76d)	30.6	VF	STL	R2	23.2	1.4
9 (44d)	31.1	VF	STL	R2	20.1	1.4

CF: Constant; VF: Variable; R1: Reactor 1 optional; R2: Aerobic; and STL: Settler.

Table 3

Reactors and settler operation parameters.

Period	MLSS R2 [mg·L⁻¹]	HRT R1+R2 [hours]	SRT R2 [days]	DO R2 [mg·L⁻¹]	External recycle	OLR-R2 [kgCOD·kgMLSS⁻¹·d⁻¹]	OFR Q_{in} [m·h⁻¹]	SL Q_{in}+Q_R [kgMLSS·m⁻²·d⁻¹]	SVI$_{30}$ [mL·g⁻¹]	TSS (out) [mL·g⁻¹]
1	3043	1.6	0.2	0.7	73%	9.9	1.3	164	64	103
2	2577	1.3	0.3	0.4	60%	8.8	1.6	155	51	92
3	1729	1.2	0.1	0.4	55%	14.9	1.7	109	55	113
4	2555	1.2	0.2	0.4	54%	8.5	1.6	156	67	119
5	2508	1.2	0.2	0.4	54%	9.8	1.6	152	48	91
6	2290	1.2	0.2	0.5	70%	9.3	0.8	79	55	66
7	2163	0.6	0.1	0.5	70%	14.6	0.8	75	59	69
8	2010	0.6	0.2	0.5	62%	10.4	0.8	65	49	65
9	1924	0.6	0.2	1.1	63%	9.5	0.8	64	49	44
Mean	2311	1.1	0.2	0.5	62%	10.6		113	55	85
S.D.	404.0	0.4	0.05	0.2	7%	2.4		43	7	25

OLR:(organic loading rate); OFR:(over flow rate); SL:(solids loading); SVI$_{30}$:(sludge volume index 30 min.).

(Eq. S3). The overflow rate (OFR) is the ratio between the pilot plant inflow and the settler surface (Eq. S4). The sludge volume index (SVI) is the ratio between the solid volume after 30 min of settling (1 L sample) and the MLSS concentration of Reactor R2. MLSS was set to maintain a constant MLSS concentration, between 2.0 and 2.2 g·L⁻¹, in Reactor R2, thus avoiding overloading in the settling tank (Eq. S5).

The organic loading rate (OLR) is the ratio between influent COD load and the inventory of the MLSS in R2 (Eq. S6). OLR were exceptionally high on Periods 3 due to the low MLSS and in Period 7, due to the high influent COD concentration.

Coarse bubbles were used in Reactor R1 only to keep the biomass in suspension and prevent the accumulation of MLSS at the bottom of the reactor. The hydraulic overflow rate was 7.14 m·h⁻¹. In turn, in Reactor R2 fine bubbles were used for both aeration and mixing. The R2 DO set point was 0.5 ± 0.2 mg·L⁻¹, similar to the half-oxygen saturation, K_{O2} (0.5 mg·L⁻¹) for AHO. The reactor temperature ranged between 18.5 and 26.3 °C without any correction. Sludge was wasted from Reactor R2 only during Period 1, and from the bottom of the settling tank during Periods 2–9. The wasting pump was run ON/OFF at a constant flow rate controlled by the MLSS concentration at the reactor R2, which had a set point of 2.000 mg·L⁻¹ without any other control variable.

The pilot plant operation, design and monitoring were based on prior simulations using the SUMO model (Hauduc et al., 2019). The SUMO model was selected because it considers the population of both OHO and AHO and the processes of adsorption and flocculation on readily biodegradable matter, i.e., VFA, monomers, polymers, and colloidal matter. The process diagram adopted in SUMO simulations, the main parameters for OHO and AHO growth and the equations to calculate operating conditions are detailed in Fig. S1 and Table S2.

2.5. COD mass balance calculation

The COD balance was calculated twice a week (on Tuesdays and Thursdays) according to the expression:

$$COD_{IN} = COD_{OUT} + COD_W + COD_{OXID} \quad (1)$$

where COD_{IN} is the influent daily flow multiplied by the average inlet COD concentration; COD_{OUT} is the effluent daily flow multiplied by the average outlet COD; COD_W is the waste daily flow multiplied by average waste COD; and COD_{OXID} is the mineralized COD. COD_{OXID}, which closes the mass balance between inlet, outlet and waste, equals the oxygen consumption. The removed COD included both the wasted and the oxidized COD, thus COD_W, is lower than the removed COD.

3. Results and discussion

3.1. Process control and operation

In order to evaluate the efficiency of the technology under different operational parameters, the HRAS-AS pilot plant was operated during 497 days over 9 different periods (Table 2 and Table 3) treating raw wastewater coming from grid and grease removal units, which constituted a significant step forward from the previous studies performed with the primary clarifiers (PC) effluent. During periods 1–3 the inflow regime was maintained constant 24h·d⁻¹, in periods 4–9 it changed according to the time table provided in Table S1. From period 7 on, only the reactor R2 was operated to evaluate the performance in the absence of the anoxic reactor R1. Finally, from period 6 on, the clarifier was changed to increase the diameter from 1 m to 1.4 m in order to analyse the influence of overflow and sludge loads in the clarifier without changing the HRT in the reactor R2.

The complexity of the HRAS technology lies in maintaining the process stability operating at such short specific SRT. In the conventional activated sludge (CAS) process, where the SRT ranges between 6 and 12 days, the reactor biomass is large enough to absorb the influent's variations. However, the short STR (<0.5 days) and HRT (R2 60 min) together with the lack of preliminary PC makes the HRAS process sensitive to the influent's variations.

Considering that there is a lack of automatic HRAS process control in previous studies, the control strategy appointed in this study was to maintain a constant MLSS reactor concentration of 2000 ± 200 mg·L⁻¹.

This low reactor MLSS concentration keeps from reactor biomass washout, lowering settling tank solid overload or prevent poor settling sludge, like in Period 3, MLSS below 1500 mg·L^{-1}. Moreover, HRAS operates at a SRT approaching the washout SRT conditions based on the maximum growth rate of biomass (Nogaj et al., 2015).

Fig. 2 shows the 24 h profile of the MLSS concentration and the waste sludge flow, both monitored through the use of in situ on-line sensors. Matching the waste sludge to the MLSS set point (2000 mg·L^{-1}) ensured the consistency and process stability, even with low SRT and HRT values. Likewise, the recirculation flow rate was set at 60% of the influent flow rate to avoid the fermentation of the biomass at the bottom of the clarifier. The oxygen concentration in reactor R2 was monitored on-line to check the efficiency of the control system. The oxidation–reduction potential (ORP) was also monitored on-line to control the reduction conditions and avoid the CH_4 generation, which leads to COD loss and greenhouse gas generation. The values ranged between −150 and −300 mV. These results are valuable knowledge in the design of a full-scale plants.

The pilot plant was running both in dry and rain weather, which highly impacts the influent COD and SS concentration. In any conditions, the peak flow rates applied to the pilot plant were as maximum 1.3 times and as minimum 0.7 times the average of the dry flow rate. It was observed that in episodes of intense rain, the extreme dilution of COD and SS influent cause a decrease in the MLSS concentration in the reactor. However, due to the low STR, the process can recover the stability within few hours.

3.2. Performance evaluation

For every experimental period, Table 4 gathers the average concentration and percentage of each COD fraction and BOD_5 in the influent together with the removal efficiency achieved. It should be noted that the removal efficiencies for each fraction indicate not only the effectiveness of the COD removal processes: adsorption, storage and oxidation but also the efficiency of the settling tank harvesting. The COD fractions and BOD_5 removal for each period is presented in Fig. 3.

As further discussed in the following sections, the average COD removal for the entire operation of the pilot plant was 57 ± 9%. COD is the sum of each COD fraction, and their weight varies constantly during the day, and in greater proportion in seasonal changes. In general terms, the removal efficiencies obtained are significantly higher than those reported in primary clarifiers (35–40%) (Crites and Tchobanoglous, 1998) and in the same magnitude to those indicated by Böhnke et al.

(Böhnke et al., 1997) (55%) for a HRAS-AS process. On the other hand, Rahman et al. (Rahman et al., 2019) reported efficiencies of 67% applying similar operational conditions but operating at a constant temperature of 20 °C, while our pilot plant operated at variable temperatures (18.5 – 26.3 °C) and it had a negative linear correlation with COD removal (Fig. 4B). The average BOD_5 removal for the entire operation of the pilot plant was 56 ± 10%, significantly higher than those reported in primary clarifiers (35–40%) (Crites and Tchobanoglous, 1998) and in the same magnitude to those indicated by Versrille et al. (Versprille et al., 1985) (55%) for a HRAS-AS process. The average results, during the whole operation, on nitrogen and phosphorus removal as TKN and TP were 21.8 ± 13.2% and 56 ± 12%, respectively. The discussion on the nutrient removal is out of the scope of this study and it will be published in a forthcoming piece.

3.2.1. Soluble COD removal efficiency

The sCOD average concentration in the raw wastewater ranged from 102 to 222 mg·L^{-1} depending on the experimental period, which accounted for and average 29% of the influent COD (Table 4), reaching values up to 32% in the Period 5. sCOD includes the soluble inert COD, the readily biodegradable volatile fatty acids (COD(VFA)), the readily biodegradable monomers (COD (mon)) and polymers (COD (poly)).

In turn, the collecting systems type: gravity, pumping, length and temperature have a determinant effect in COD fractions. According to Wilén et al. (2006), the biological processes in the sewer system are predominantly aerobic in high flows and anaerobic in low flows, thus changing wastewater properties. Moreover, in an anaerobic sewer collection system, the temperature promotes an increase in fermentation rates and in turn increased the sCOD removal. Likewise, the temperature increases the COD(VFA) and COD(mon) fraction stored by AHO organisms. Hauduc et al. (2019) reported that at 20 °C COD(mon) was ca. 60% of the sCOD, while at 15 °C, COD(mon) was ca. 40% of the sCOD.

The sCOD removal efficiency achieved in the HRAS pilot plant had an average value of 29±12%, ranging between 19±13% and 36±9% depending on the experimental period. These results are in the same order than those indicated by Miller (2015), 33±12%, and by De Graaff et al. (2016), 11 ± 61%. Jimenez et al. (2015) achieved a sCOD removal of 50–60% working at a DO concentration of 1.0 mg·L^{-1} and higher SRT of 1 day.

In order to investigate the sCOD influent concentration effect over the sCOD removal efficiency, Fig. 4 shows the relation between COD_{in} fractions and the COD removal at 20 °C corrected temperature (Θ=1.045) (Seeley, 1992) along the nine experimental periods
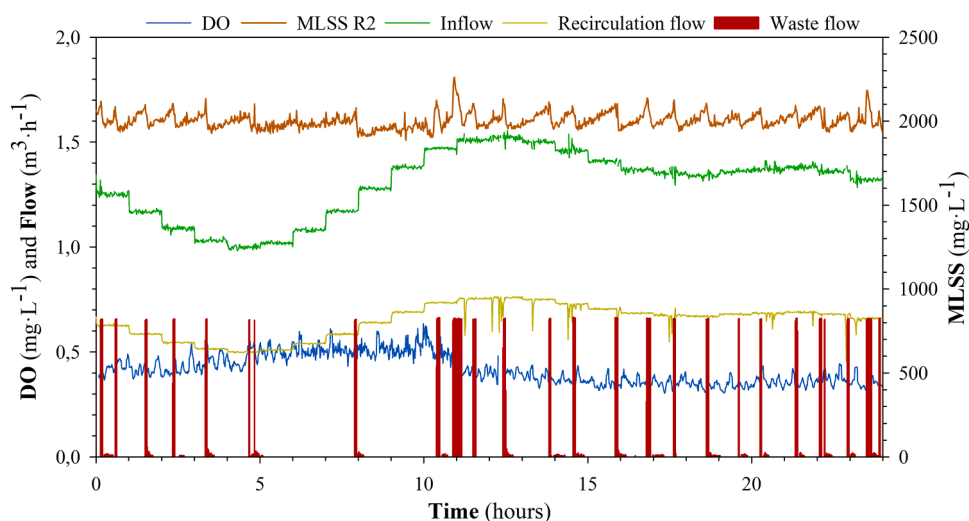

Fig. 2. 24 h monitoring of the process control parameters: waste sludge flow rate and MLSS concentration in reactor R2, dissolved oxygen (DO) and recirculation flow rate.

Table 4

COD fraction concentration averages at influent and removal in each experimental period.

Period	$sCOD_{IN}$ [mg·L^{-1}] *(COD%)	sCOD (rem) [%]	$cCOD_{IN}$ [mg·L^{-1}] *(COD%)	cCOD (rem) [%]	$pCOD_{IN}$ [mg·L^{-1}] *(COD%)	pCOD (rem) [%]	Total COD_{IN} [mg·L^{-1}]	COD (rem) [%]	BOD_{5IN} [mg·L^{-1}]	BOD_5 (rem) [%]
1	180 (18%)	27 ± 12	61 (6%)	−4 ± 38	766 (76%)	81 ± 7	990	66 ± 10	455	67 ± 14
2	183 (28%)	30 ± 13	61 (9%)	9 ± 25	419 (63%)	78 ± 10	658	57 ± 8	283	51 ± 13
3	187 (27%)	31 ± 11	59 (9%)	8 ± 36	438 (64%)	72 ± 8	684	55 ± 7	261	57 ± 8
4	161 (27%)	34 ± 9	69 (11%)	24 ± 20	372 (62%)	61 ± 9	602	50 ± 6	244	50 ± 12
5	222 (32%)	36 ± 9	60 (9%)	16 ± 32	401 (59%)	73 ± 8	680	56 ± 9	257	58 ± 5
6	168 (29%)	24± 12	50 (9%)	4 ± 33	372 (62%)	77 ± 8	585	55 ± 7	212	49 ± 7
7	200 (23%)	28 ± 5	83 (10%)	62 ± 11	570 (67%)	75 ± 13	853	63 ± 12	401	58 ± 3
8	138 (23%)	23 ± 11	69 (12%)	16 ± 47	381 (65%)	71 ± 13	588	53 ± 13	204	54 ± 11
9	102 (19%)	19 ± 13	54 (10%)	12 ± 32	359 (71%)	77 ± 6	515	59 ± 6	160	57 ± 13
Average	171 (25%)	29 ± 12	62 (9%)	12 ± 35	453 (66%)	74 ± 10	683	57 ± 9	254	56 ± 10

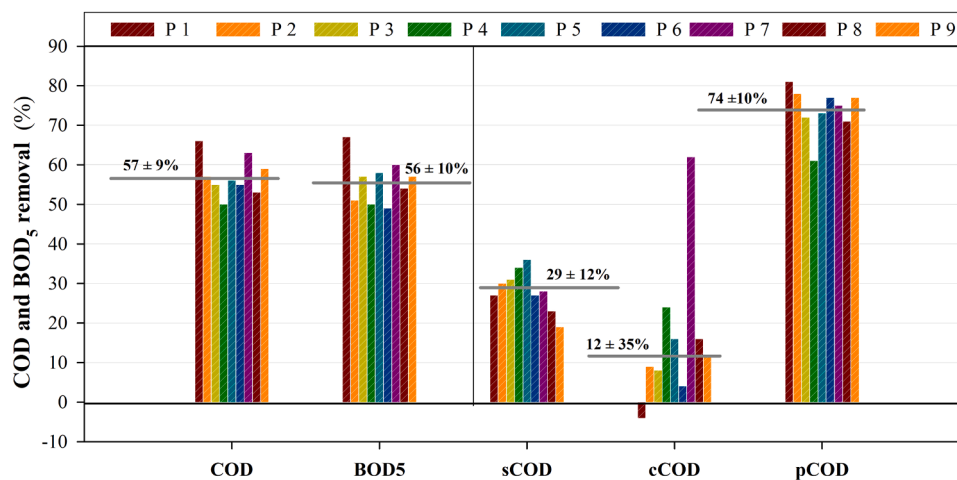[*] COD fraction percentage regarding total COD.

Fig. 3. COD and BOD_5 average removal efficiencies for each period. The horizontal line marks the average removal for the entire operation of the pilot plant and the associated standard deviation.
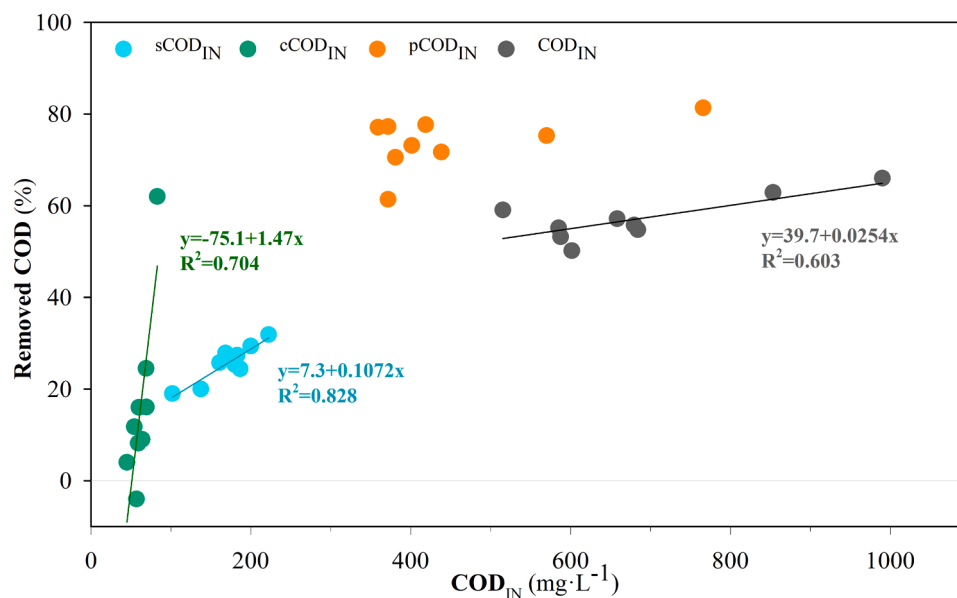

Fig. 4. sCOD, cCOD, pCOD and COD removal percentage related to their influent concentration.

considered. The good correlation indicated that the sCOD removal was controlled by a biological oxidation-storage process according to Hauduc et al. (2019). At time, Fig. 5A shows, for each period, the sCOD

removal, the temperature and $sCOD_{in}$ concentration. It can be highlighted that for the same $sCOD_{in}$ the temperature increase, promoted the increase of the sCOD removal: Periods 6 and 4 had similar $sCOD_{in}$ (168
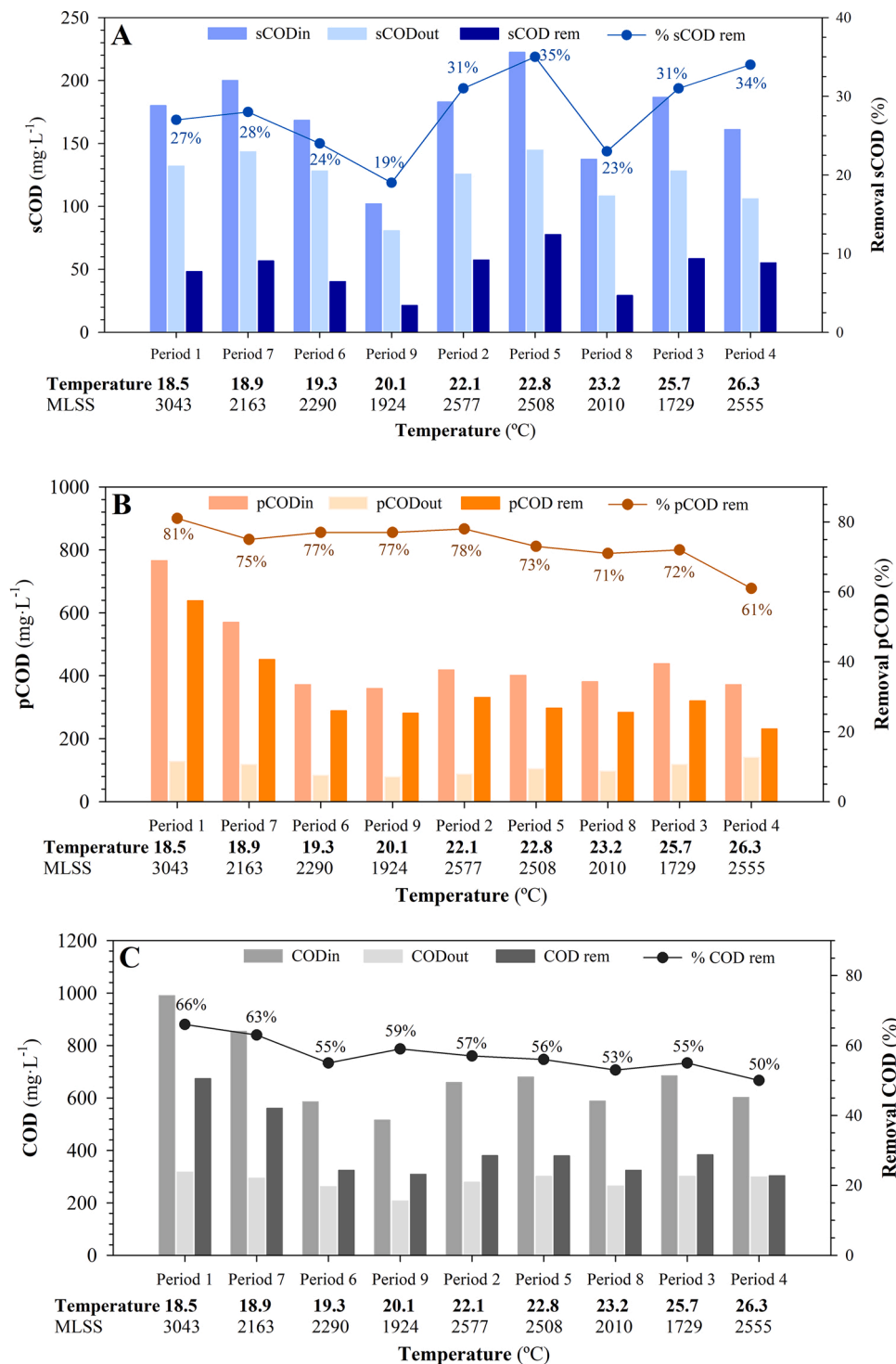
Fig. 5. Influent, effluent and removal of COD fractions based on temperature. A) sCOD, B) pCOD and C) COD.

mg·L^{-1}) and a temperature difference of 7°C, leading to an increase of 10% removal. However, periods 1 and 3, had similar sCOD$_{in}$ (180 mg·L^{-1}) and a temperature difference of 7°C, but the removal increase was only 4% probably due to the lower MLSS concentration in Period 3.

The relation between MLSS concentration in the R2 and the sCOD removal efficiency was investigated at 20 °C corrected temperature (Θ=1.045). The results for each operational period are shown in Fig. S2, where it can be observed that periods 3, 2 and 1 with similar sCOD$_{in}$ and a MLSS concentration of 1729 mg·L^{-1}, 2577 mg·L^{-1} and 3.000 mg·L^{-1} respectively, presented sCOD removal efficiencies of 24%, 27% and

29% respectively.

Finally, the elimination of the anoxic reactor R1 in periods 7, 8 and 9, confirmed the non-affectation of reactor R1 in sCOD removal.

3.2.2. Colloidal COD removal efficiency

The cCOD average concentration in the raw wastewater ranged from 54 to 83 mg·L^{-1} depending on the experimental period, which accounted for and average 9% of the influent COD. In general terms, the removal of cCOD was between −4 and 24% (Table 4), with a noticeable increase during period 7 which corresponds to a significant increase in

the inlet cCOD. The effect of the inlet cCOD with the removal efficiency was investigated, resulting a first-order kinetics shown in (Fig. 4A) where the higher the inlet, the more removal efficiency, unlike that indicated by Bunch and Griffin (Bunch and Griffin Jr., 1987), who proposed zero-order kinetics.

It is important to highlight that during the first operational stage, the results led to negative cCOD removal due to the fact that the deflocculation produced by the high recirculation pumping was higher than the flocculation process to remove cCOD. In the design of the HRAS process equipment, such as pumps and agitators, the minimization of this deflocculation effect must be taken into account. Increased cCOD in the effluent was also reported by Miller (2015) (negative removals of 28%) due to the conversion of sCOD into non-flocculated colloidal biomass, and by Bisogni (James Bisogni and Lawrence, 1971) at short SRTs as a result of dispersed biomass growth. HRAS has been observed as bio-flocculation limited by low cCOD removal efficiency, which may potentially be due to lack of (EPS) production (Kinyua et al., 2017). Likewise, decay processes and large clarifier hydraulic retention times can produce colloidal material (Hauduc et al., 2019).

3.2.3. Particulate COD removal efficiency

The pCOD constituted the major part of the inlet COD (66%), with an average influent concentration of 453 mg$\cdot L^{-1}$, ranging from 359 to 766 mg$\cdot L^{-1}$ depending on the experimental period (Table 4). The removal of the pCOD, which controls the overall COD removal because of its largest contribution, is associated with the adsorption onto biomass flocs by electrostatic interactions due to the biological activity. Moreover, the settling characteristics are determining in the HRAS process for the gravity separation of particulate matter.

The relationship between pCOD removal over the nine experimental periods and the following variables: solid loading (SL), overflow rate (OFR), pCOD$_{IN}$ concentration, MLSS and temperature are show in Fig. 5. The solids loading (SL) did not affect pCOD removal due to the high sludge settling properties, low SVI30 (49–67 mL$\cdot g^{-1}$) (Table 3), compared to (110–180 mL$\cdot g^{-1}$) in CAS processes (Seeley, 1992) and similar to the values reported by Böhnke et al. (1997) (40–90 mL$\cdot g^{-1}$), Miller (2015) (85±26 mL$\cdot g^{-1}$), Van Winckel et al. (2019) (88±81 mL$\cdot g^{-1}$) and Rahman et al. (2019) (88±18 mL$\cdot g^{-1}$) in their HRAS pilot plant studies. Furthermore, the variation in the SL did affect the effluent suspended solid (SS) concentration (Fig. 6A), although its impact was also linked to the variation in the overflow rate (OFR). At turn, OFR did not affect pCOD (Fig. 6B) removal due to the high sludge settling properties. The variation of the OFR did, however, affect the effluent suspended solid SS$_{OUT}$ concentration, although its impact was also linked to the variation in SL (Fig. 6A).

The pCOD$_{IN}$ concentration had slight effect on the pCOD removal

efficiency (Fig. 4). Period 4, with an average pCOD removal efficiency of only 61%, corresponded mainly to August. The combination of both low pCOD$_{IN}$ load and the high temperature (26.3 °C) of this period explains the low efficiency achieved. pCOD removal remained at high values (70–80%), regardless of the pCOD$_{IN}$ concentration.

At time, Fig. 5B shows, for each period, the pCOD removal, the temperature and the pCOD$_{in}$ concentration. It can be highlighted that for a given pCOD$_{in}$, the temperature increase promoted a decrease of the pCOD removal: Comparing Periods 6, 8 and 4, at similar pCOD$_{in}$ (372 mg$\cdot L^{-1}$) and MLSS concentration of 2290 mg$\cdot L^{-1}$, 2010 mg$\cdot L^{-1}$ and 2555 mg$\cdot L^{-1}$ respectively, and a temperature variation of 19.3°C 23.2°C and 26.3°C resulted on a pCOD removal of 77%, 71% and 61% respectively suggesting that temperature has a negative contribution on pCOD removal.

On the one hand, as previously indicated by Jorand et al. (1995), temperature does not affect the pCOD bioadsorption process; on the other hand, increasing the temperature leads to a decrease in the viscosity of the medium and should, consequently, cause better settling of the biological flocs. The behaviour observed may be related to the increased hydrolysis and decay process rate with temperature (Nogaj, 2015; Takács, 2021), i.e. the redissolution of the pCOD into the settling tank. Another factor that produces an increase in hydrolysis is the continuous arrival of OHO heterotrophic organisms in the influent from the internal return line. However, here, other processes seem to be occurring. Most likely, the viscosity of the sludge decreases with increasing temperature, which results in less efficient particle capture in the settler.

The MLSS concentration in the reactor had a good correlation with the pCOD removal for all periods (Fig. S3) since it promoted the flocculation and entrapment of particulate matter in biological flocs (Hauduc et al., 2019), e.g. pCOD removal efficiency was 6% higher in period 2 (MLSS 2577 mg$\cdot L^{-1}$) than in period 3 (MLSS 1729 mg$\cdot L^{-1}$). Nevertheless, the biomass activity in a HRAS process without primary clarifier, is not as constant as in a CAS process, and its characteristics are highly affected by the concentration and composition of the influent SS. For a MLSS concentration below 1500 mg$\cdot L^{-1}$ the settling began to worsen. The control system implemented in the pilot plant maintained MLSS at 2312 ± 404 mg$\cdot L^{-1}$, thus promoting pCOD removal efficiency.

Considering that the SRT values were practically constant during the whole operation and that the EPS content depends on the SRT applied (Rahman et al., 2016), the analysis of the EPS production and its effects were out of the scope in this study. Previous studies did not identified a significant influence of EPS on the bioflocculation and settling at short SRTs (Elliot, 2016; Kinyua et al., 2017). Moreover, the HRAS removed the pCOD that would had been removed in a primary clarifier regardless of the biological activity
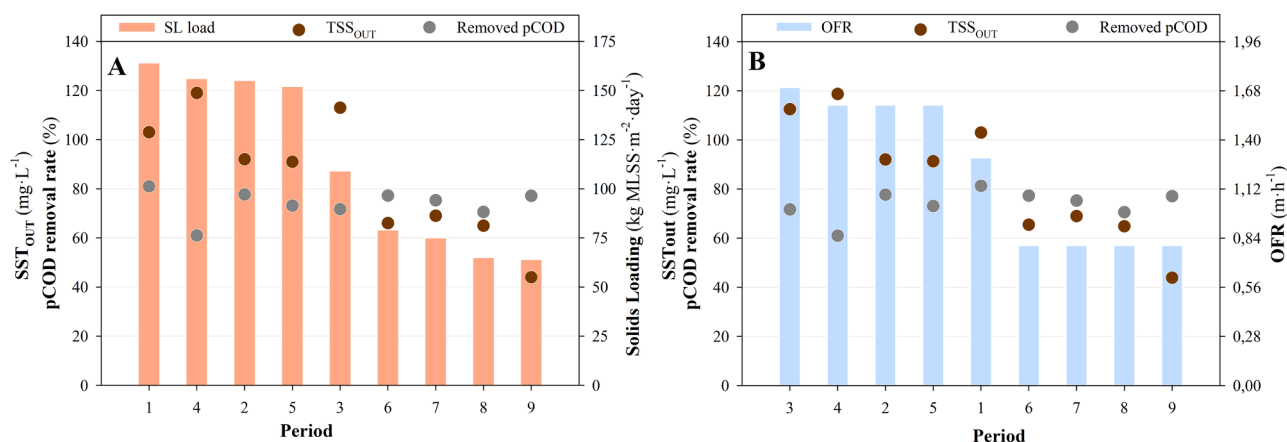

Fig. 6. A) Relationship between solid loading, pCOD removal percentage and SS$_{OUT}$. B) Relationship between overflow rate and pCOD removal percentage and SS$_{OUT}$.

In summary, the variables exerting the greatest effect on pCOD removal were the temperature, the $pCOD_{in}$ and the MLSS concentration in the aerobic reactor (R2). The OFR and SL in the settling tank had a minor impact on the pCOD removal. The pCOD removal efficiency was higher than a value of 65% reported by Jimenez et al. (2015) with a SRT of 0.5 days and DO of 0.5 mg·L^{-1} and was also higher than a value of 55% reported by Miller et al. (2013). The above confirms the robustness and success of the automatic control strategy, which maintained a fixed MLSS concentration in the reactor. This is to be noted, since this is the first study operated at a quite constant MLSS that achieved such high removal efficiencies.

3.2.4. Total COD

COD removal is the sum of each COD fraction's removal. The weight of each COD fraction changes constantly during the day and in greater proportion in seasonal periods. COD_{IN} concentration had a good correlation with COD removal (Fig. 4). Temperature effect that on pCOD removal (Fig. 5B), which was not offset by the positive effect on sCOD removal (Fig. 5A) because the pCOD fraction was much higher than the sCOD fraction. The increase of biomass concentration in the reactor led to a slight increase of the pCOD and thus COD removal efficiency (Fig. S4).

As a summary, it is important to highlight the correlation between influent COD fractions and COD fractions removal. As shown in Fig. 4, the cCOD removal presented highly dispersed values for a minimum variation in low influent concentrations (30–60 mg·L^{-1}), the sCOD removal presents less dispersed values for a high range of influent concentrations (40–250 mg·L^{-1}), and the pCOD removal present a minimal dispersion values for a high range of influent concentrations (350–800 mg·L^{-1}). This highlights the importance of pCOD removal, like remarked by Guven et al. (2019) and, to a lesser extent of sCOD removal. The high dispersion of cCOD removal values and the low weight of cCOD in the total COD make this COD fraction the least important in the control of the HRAS process.

From the standpoint of energy recovery, the key point is to harvest as much COD as possible (Guven et al., 2019a). Nevertheless, it is critical to differentiate the removal of each COD fraction given their importance in the subsequent nitrification–denitrification process. An increase of soluble COD in effluent HRAS would result in a quickly removal during the aerobic cycle, thus decreasing the COD available for denitrification in the anoxic cycle (Regmi et al., 2014).

As a novelty of this study, the COD fractions removal analysis has been additionally carried out in periods of six hours. Fig. S5 shows the sCOD and pCOD in the influent load and in the effluent for each 6-hour period, together with the amount removed. In periods 13h-18 h and 19h-24 h, the sCOD and pCOD load increased compared to periods 01h-06 h

and 07h-12 h. While the sCOD remained constant during the day ca. 90 g·h^{-1}, the pCOD removed increased with the pCOD load. More detailed hourly monitoring will be of interest in further development of the HRAS technology.

3.3. Effect of SRT over COD removal

The HRAS pilot plant was operated with the goal to maintain the MLSS constant as process control parameter. The SRT (0.1–0.4 days) resulting from the MLSS control was correlated with COD removal efficiency to evaluate the effect of the SRT on the system performance. Fig. 7 shows the correlation between STR and each COD fraction removal during the whole operation time, with data divided into the different ranges of temperature conditions. It can be observed that there is no correlation in any case, indicating that SRT value was not a determining factor in COD fractions removal, at so low SRT, which is in agreement with the conclusions reported by Rahman et al. (2017).

3.4. COD mass balance

The COD mass balance was calculated for each experimental period in order to investigate the efficiency of the process in terms of COD sent to digestion and COD oxidized. Fig. 8 shows the results of the mass balance for each period. In general terms, the oxidation was low, under the values reported by Haider et al. (2003) (12% COD_{OXID} at STR 0.1 d),
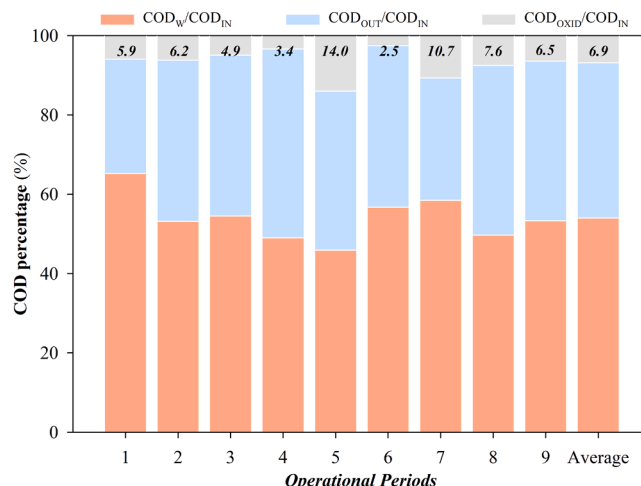
Fig. 8. COD influent mass balance distribution: waste, out and oxidized.
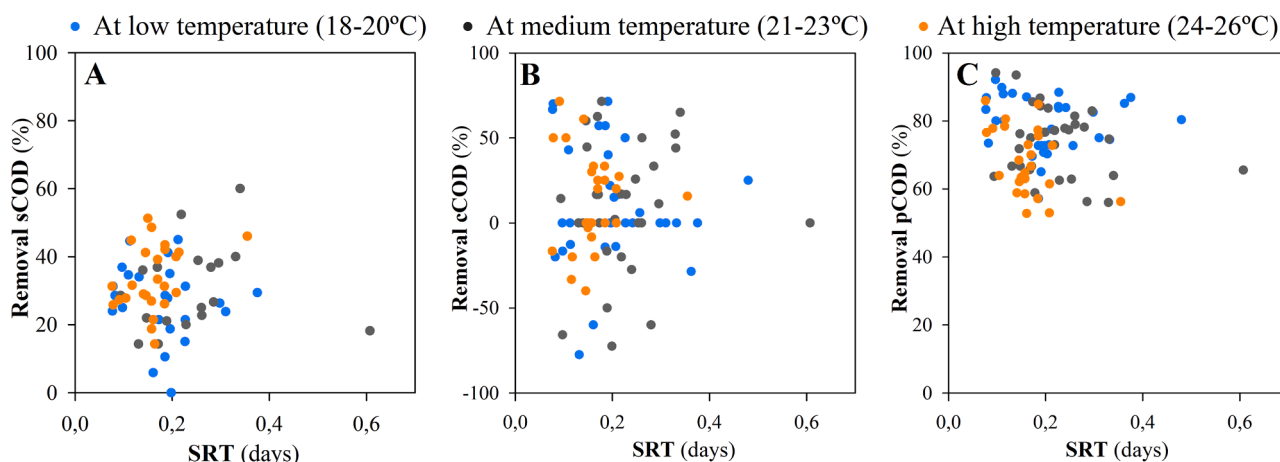
Fig. 7. SRT and COD fractions removal at 18–20 °C, 21–23 °C and 24–26 °C. A) sCOD, B) pCOD and C) COD.

Miller et al. (2017) (14% COD$_{OXID}$ at STR1 d) and (Taboada-Santos et al., 2020) (16% COD$_{OXID}$ at STR 0.9 d).

Thus, the HRAS working at low SRT (0.2 ± 0.05d), low DO (0.5 ± 0.2 mg·L^{-1}) and the already reported high variations in the influent load, permitted to send to digestion an average 55% of the influent COD, with a low average oxidation of 6.9 ± 3.6% and maintaining the COD$_{OUT}$ around 40% for almost every period.

3.5. BOD$_5$ removal

BOD$_5$ removal follows the same pattern than COD removal, presented in Fig. S6A. The COD and BOD$_5$ removal rates were similar: 57±9% and 56±10% respectively (Table 4). Fig. S6B presents the correlation between COD and BOD$_5$ removed, approximately 38% of COD removed was BOD$_5$. Likewise, the BOD$_5$/COD ratios in the influent and effluent were the same, 40% and 40%, respectively, indicating no variation in water degradability features.

Overall, the HRAS influent and effluent concentrations of COD, COD fractions and BOD$_5$ for each period are presented in Fig. S7. As it has been noted before (Section 3.2) the BOD$_5$ removal efficiencies also include BOD$_5$-carbon redirection process (adsorption, storage and oxidation) and also the BOD$_5$-carbon harvesting process (settling and waste). Figs S6 and S7 also indicate the high sCOD, pCOD, COD and BOD$_5$ removal and the buffering capacity of HRAS process.

3.6. Long-term stability evaluation

After analysing the average removal efficiencies of each period for the different COD fractions, Fig. 9 and 10 show the daily evolution of COD$_{IN}$ and COD$_{OUT}$ throughout all the experimental time for each COD fraction and BOD5. It can be observed that the HRAS process did not act as a filter for sCOD$_{IN}$ peak loads (Fig. 9A), as it did for pCOD (Fig. 9B), since the high dispersion in sCOD$_{IN}$, 171±61 mg·L^{-1}, was matched by a high dispersion in sCOD$_{OUT}$, 121±44 mg·L^{-1}. On the contrary of pCOD

(Fig. 10B), there was not a clear correlation between the inlet concentration of sCOD and the removal efficiency (Fig. 10A). The maximum sCOD removed was 140 mg/L, regardless of the influent concentration, since similar absolute removal value was achieved at inlet concentration of 230, 290 and 380 mg/L. Thus, the system presented a maximum sCOD removal capacity, as usual of biological processes.

However, the HRAS process acted as a filter for pCODin peak loads (Fig. 9B), buffering the loads to the subsequent activated sludge process. Even with the high dispersion in pCODin (456±200 mg·L^{-1}) the pCODout values presented a low dispersion (106±34 mg·L^{-1}), and the maximum and average values of pCOD removal were 1280 and 349 ±198 mg·L^{-1}, respectively. The almost totally parallel relationship between the pCOD removal regression line and the line representing the total pCODin removal, dotted line (Fig. 10B) indicates the presence of a non-settling pCOD that could not be removed and was independent of the pCODin concentration.

Accordingly, the HRAS process acted as a filter for CODin peak loads (Fig. 9C), buffering the inlet loads to the subsequent activated sludge process. There was a high dispersion in CODin (683±214 mg·L^{-1}) that was buffered in the process with a low dispersion in CODout (280±63 mg·L^{-1}), thus, buffering the organic loads to the subsequent activated sludge process. The maximum and average COD removal values were 1300 and 403±195 mg·L^{-1}, respectively. The almost total parallel relationship between the regression line of COD removal and the line representing total CODin removal, dotted line (Fig. 10C) indicates that a constant amount of COD could not be removed and independently from the CODin concentration. This non-removable COD included non-settling pCOD, sCOD (poly) and non-flocculated cCOD under the pilot plant's operating conditions. Hence, the overall COD removal efficiency was lower due to the lower sCOD removal efficiency in comparison with the pCOD removal efficiency. Improvement on COD removal could only be achieved by either increasing sCOD oxidation, with the consequent energy consumption, or by improving the pCOD removal associated with improved settling.
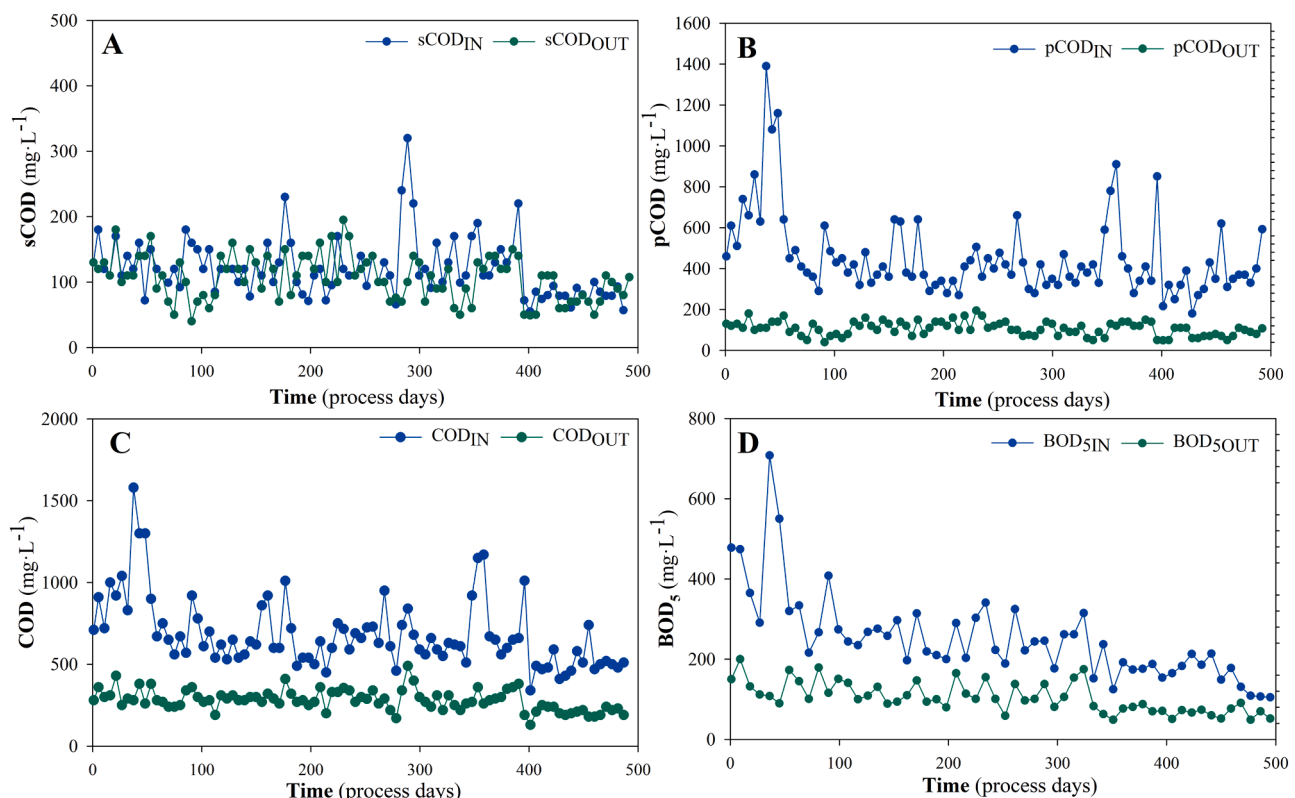

Fig. 9. Daily variations of the influent and effluent concentrations of A) sCOD; B) pCOD; C) COD and D) BOD$_5$.
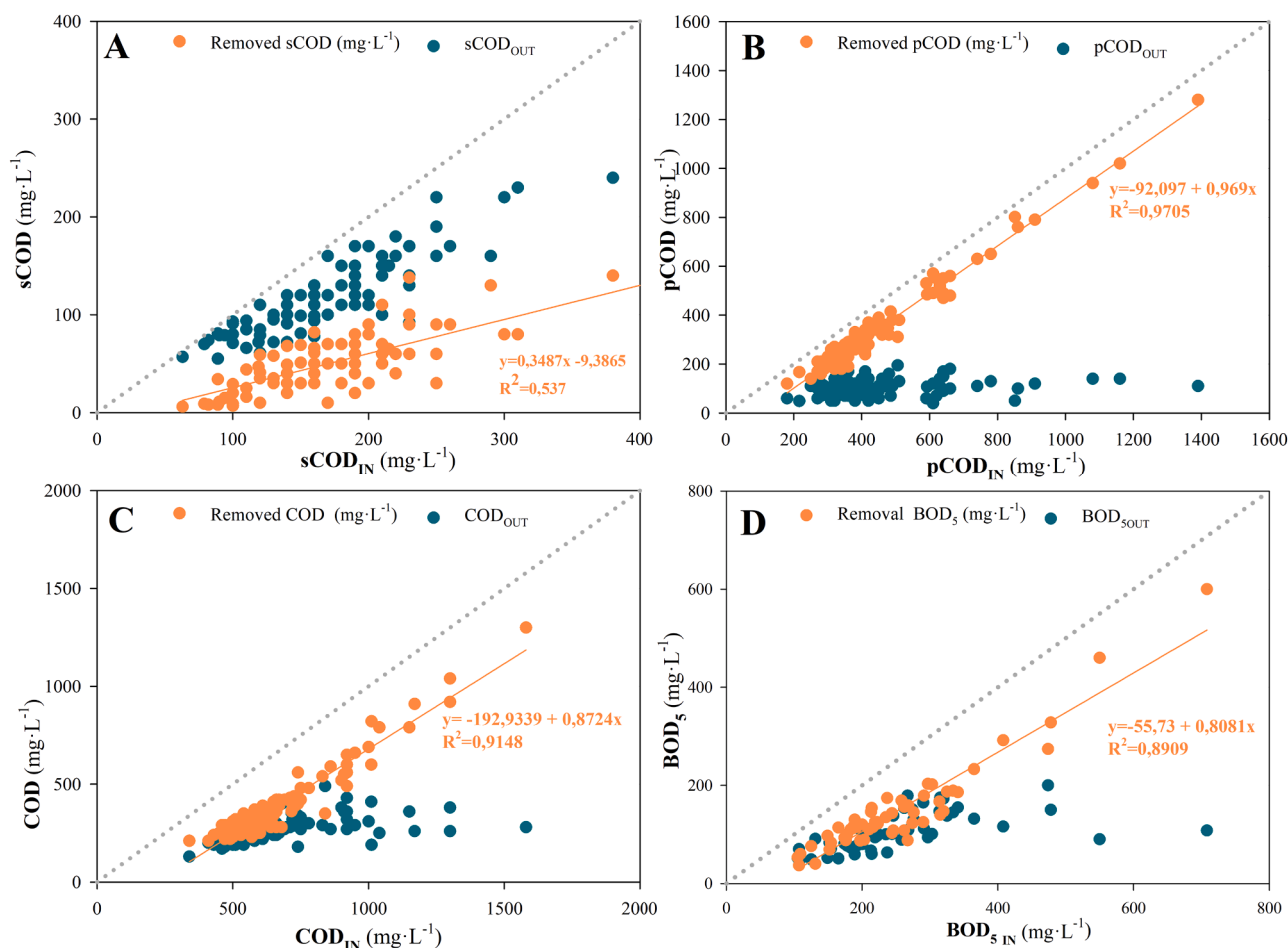
Fig. 10. Relation between the removed, influent and effluent concentrations of A) sCOD, B) pCOD, C) COD and D) BOD$_5$.

Regarding the BOD$_5$ loading, the HRAS process acts as a filter for BOD$_5$ in peak loads (Fig. 9D) and it buffers the organic loads to the subsequent activated sludge process. The high dispersion in BOD$_5$in (253 ± 110 mg·L^{-1}) is matched by a low dispersion in BOD$_5$out (112 ± 59 mg·L^{-1}). The maximum and average values of BOD$_5$ removal were 600 and 154 ± 95 mg·L^{-1}, respectively.

The almost total parallel relationship between the regression line of BOD$_5$ removal and the line representing total BOD$_5$ removal, dotted line (Fig. 10D) indicates the presence of a BOD$_5$ that could not be removed, which includes the non-settling BOD$_5$ and the nonbiodegradable BOD$_5$ at short HRT. Increased BOD$_5$ removal could be by achieved by increasing biodegradation, with the consequent energy consumption, or by improving the removal of particulate BOD$_5$, which is associated with improved settling, as indicated for COD.

Overall, the HRAS process made it possible not only to send larger amount of organic matter to anaerobic digestion (58–60% of the CODin and 49–67% of the BOD5in) compared to the 35–40% achieved with primary clarifier (Crites and Tchobanoglous, 1998) but also to laminate the influent load to the activated sludge unit, assuring its stability and reducing the size of the equipment to be installed in the unit to handle oxygen demand peaks.

3.7. Process simulation

Process simulations were carried out by means of Sumo-19 software, according to the model configuration detailed in the Fig. S1 with the goal of testing its capability to predict the removal efficiency of the different COD fractions. The main parameters used in the model for the growth of ordinary heterotrophic organisms (OHO) and A-stage fast-

growing microorganisms (AHO) are shown in the Table S2. The COD fractions used were determined according to the average values of the pilot plant for each period. The sCOD split and OHO and AHO fraction in the influent total COD were determined according to the default values of the model.

In comparison with full scale facilities, the pilot plant has two specific characteristics: low flocculation in the reactor due to wall effects, and low deflocculation in the recirculation line due to the use of helicoidal pumps at low speed, instead of centrifugal pumps at higher speed. Thus the most sensitive parameters to be adjusted were the flocculation reduction factor in the reactor $\eta_{FLOC,Process}$ – to a value of 0.4 (Reactor R1) and 0.2 (Reactor R2) – and the deflocculation factor in the recirculation line to a value of 10%. The first parameter combines all hydrodynamic effects affecting the shear force on the flocs (reactor geometry, type of aerators and mixers) that act on the residual colloids, and the second parameter refers to the deflocculation factor in the recirculation line (Hauduc et al., 2019). A reactive three-compartment clarifier with a 0.9 flocculation factor in the feed well and sludge blanket was used for the settling model.

Fig. 11 presents the efficiencies obtained in the pilot plant versus the predicted with the model. sCOD, cCOD and pCOD removal efficiencies were closely predicted by the model as a function of their corresponding inlet concentrations with additional indication of the temperature.

For sCOD$_{IN}$ values above 183 mg·L^{-1}, the efficiency in the pilot plant was higher than that calculated in the model, and for values below 180 mg·L^{-1}, the efficiency in the model was higher than that obtained in the pilot plant (Fig. 11A). A possible explanation for this is the fact that the saturation constant for the biodegradable organic substrate Ks used (default constant in the model) was lower than the real value. As
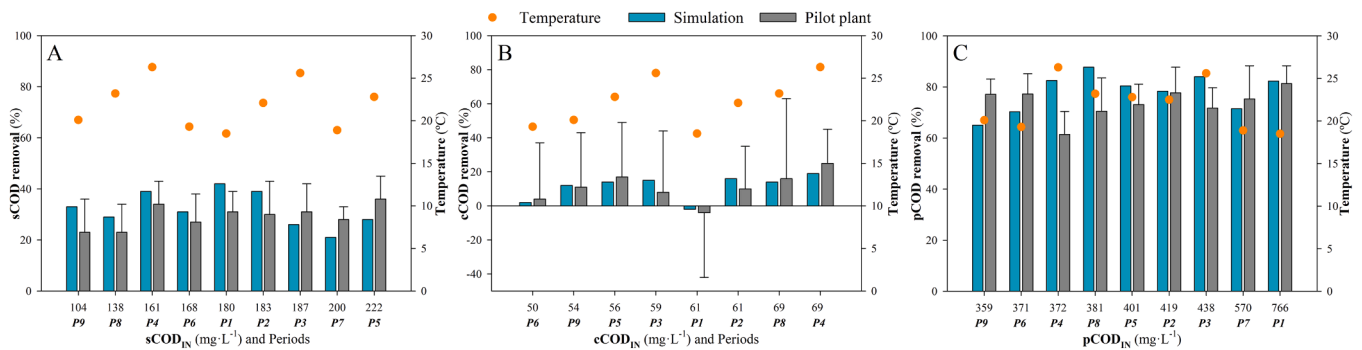
Fig. 11. Removal efficiencies obtained by simulation and pilot plant: A) sCOD, B) cCOD and C) pCOD.

shown in Fig. 11B, the cCOD removal efficiencies were closely predicted by the model as function of the cCODin concentration. However, the large deviation in the experimental results of the cCOD data must be considered when analysing the model outcomes. Finally, for pCOD simulation, the model differs from the pilot plant results for temperatures above 23 °C (Fig. 11C), which is aligned with the reduction of pCOD removal efficiency observed in the pilot plant at highest temperatures (Fig. 4B).

In this study, the model was tested against HRAS-A stage pilot plant operation data and proven to match the COD fraction removal efficiency. Future research should supplement the current study with a thorough examination of nutrient removal efficiencies in both short- and long-term HRAS processes, as well as a COD balance and oxygen uptake rates.

Conclusions

Reducing SRT up to 0.2 days and HRT up to 0.6 h, corresponding to one third of the usual values reported in HRAS operation, allows a high redirection and harvesting of organic matter (57±9%) for COD and (56 ±10%) for BOD$_5$, with a minimum 6.9% COD oxidation. The different COD fraction removal: (29±12%) sCOD, (12±35%) cCOD and (74 ±10%) pCOD, highlights the importance of settling efficiency and stability in the HRAS removal efficiencies.

Maintaining the biomass concentration in the reactor at 2000±200 mg$\cdot L^{-1}$ as process control strategy assured a very stable process even with the large variations in the influent. So, both in short- and long-term performance the best control parameter at very low SRT to ensure the process stability and minimize COD oxidation is not strictly the SRT but rather the MLSS concentration.

The biomass concentration was directly correlated with sCOD and pCOD removal, while reactor temperature hampered the pCOD removal but increased sCOD. The direct relation between influent COD concentration and COD removal makes it advisable to use the HRAS process as a replacement of the PC stage and not as a downstream treatment afterward.

Settling efficiency and stability showed a great importance in the HRAS performance. The low SVI$_{30}$ values of 50–70 ml$\cdot g^{-1}$ shows the exceptional biomass settling properties, while the relatively low SS effluent concentration 50–120 mg$\cdot L^{-1}$ indicated correct flocculation.

HRAS-AS process acts as a filter for the influent COD and pCOD peak loads and, albeit to a lesser extent, for BOD$_5$, buffering the influent load to the subsequent CAS process. The HRAS-AS process, on the other hand, does not act as a filter for sCOD peak loads, which is important regarding the likely subsequent denitrification process. The simulation model adopted (SUMO) resulted in a good fit for the sCOD. For pCOD, there was a good fit except for temperatures above 23 °C.

Declaration of Competing Interest

The authors declare that they have no known competing financial interests or personal relationships that could have appeared to influence the work reported in this paper.

Data Availability

Data will be made available on request.

Supplementary materials

Supplementary material associated with this article can be found, in the online version, at doi:10.1016/j.watres.2023.119610.

References

APHA, 2005. Standard Methods for the Examination of Water and Wastewater, 21st ed. American Public Health Association (APHA), American Water Works Association (AWWA) & Water Environment Federation (WEF), Washington DC.

Böhnke, B., Diering, B., Zuckut, S., 1997. Cost-effective wastewater treatment process for removal of organics and nutrients - ScienceBase-Catalog. Water Eng Manag 144, 18–21.

Bunch, B., Griffin Jr., D.M., 1987. Rapid removal of colloidal substrate from domestic wastewaters on JSTOR. J. Water Pollut. Control Fed. 59, 957–963.

Carrera, J., Carb.., O., Do..ate, S., Su..rez-Ojeda, M.E., P..rez, J., 2022. Increasing the energy production in an urban wastewater treatment plant using a high-rate activated sludge: Pilot plant demonstration and energy balance. J. Clean. Prod. 354, 131734. https://doi.org/10.1016/j.jclepro.2022.131734.

Christian, S.J., Grant, S.R., Singh, K.S., Landine, R.C., 2008. Performance of a high-rate/ high-shear activated sludge bioreactor treating biodegradable wastewater. Environ. Technol. 29, 837–846. https://doi.org/10.1080/09593330801987616.

Constantine, T., Houweling, D., Kraemer, J., 2012. Doing the two-step" – Reduced energy consumption sparks renewed interest in multistage biological treatment. In: WEFTEC 2012 - 85th Annual Technical Exhibition and Conference. Water Environment Federation, pp. 5771–5783. https://doi.org/10.2175/193864712811709652.

Crites, R., Tchobanoglous, G., 1998. Small and Decentralized Wastewater Management Systems. WCB/McGraw-Hill.

De Graaff, M.S., Van Den Brant, T., Roest, K., Van Den Brand, T.P.H., Roest, K., Zandvoort, M.H., Duin, O., Van Loosdrecht, M.C.M., Van Den Brant, T., Roest, K., 2016. Full-scale highly-loaded wastewater treatment processes (A-stage) to increase energy production from wastewater: performance and design guidelines. htt ps://home.liebertpub.com/ees 33, 571–577. https://doi.org/10.1089/ EES.2016.0022.

Elliot, M.S., 2016. Impacts of operating parameters on extracellular polymeric substances production in a high rate activated sludge system with low solids retention times. Civ. Environ. Eng. Theses Diss. https://doi.org/10.25777/5mmx-c139.

Guven, H., Ersahin, M.E., Dereli, R.K., Ozgun, H., Isik, I., Ozturk, I., 2019a. Energy recovery potential of anaerobic digestion of excess sludge from high-rate activated sludge systems co-treating municipal wastewater and food waste. Energy 172, 1027–1036. https://doi.org/10.1016/j.energy.2019.01.150.

Guven, H., Ozgun, H., Ersahin, M.E., Dereli, R.K., Sinop, I., Ozturk, I., 2019b. High-rate activated sludge processes for municipal wastewater treatment: the effect of food waste addition and hydraulic limits of the system. Environ. Sci. Pollut. Res. 26, 1770–1780. https://doi.org/10.1007/s11356-018-3665-8.

Haider, S., Svardal, K., Vanrolleghem, P.A., Kroiss, H., 2003. The effect of low sludge age on wastewater fractionation (SS, SI). Water Science and Technology. IWA Publishing, pp. 203–209. https://doi.org/10.2166/wst.2003.0606.

Hauduc, H., Al-Omari, A., Wett, B., Jimenez, J., De Clippeleir, H., Rahman, A., Wadhawan, T., Takacs, I., 2019. Colloids, flocculation and carbon capture – a comprehensive plant-wide model. Water Sci. Technol. 79, 15–25. https://doi.org/ 10.2166/WST.2018.454.

Huang, J.C., Li, L., 2000. Enhanced primary wastewater treatment by sludge recycling. J. Environ. Sci. Heal. - Part A Toxic/Hazardous Subst. Environ. Eng. 35, 123–145. https://doi.org/10.1080/10934520009376958.

James Bisogni, J., Lawrence, A.W., 1971. Relationships between biological solids retention time and settling characteristics of activated sludge. Water Res. 5, 753–763. https://doi.org/10.1016/0043-1354(71)90098-4.

Jia, M., Solon, K., Vandeplassche, D., Venugopal, H., Volcke, E.I.P., 2020. Model-based evaluation of an integrated high-rate activated sludge and mainstream anammox system. Chem. Eng. J. 382, 122878 https://doi.org/10.1016/J.CEJ.2019.122878.

Jimenez, J., Miller, M., Bott, C., Murthy, S., De Clippeleir, H., Wett, B., 2015. High-rate activated sludge system for carbon management - Evaluation of crucial process mechanisms and design parameters. Water Res. 87, 476–482. https://doi.org/ 10.1016/j.watres.2015.07.032.

Jorand, F., Block, J.-.C., Palmgren, R., Nielsen, P.H., Urbain, V., Manem, J., 1995. Biosorption of wastewater organics by activated sludges. Récents Progrès En Génie des Procédés.

Kinyua, M.N., Elliott, M., Wett, B., Murthy, S., Chandran, K., Bott, C.B., 2017. The role of extracellular polymeric substances on carbon capture in a high rate activated sludge a-stage system. Chem. Eng. J. 322, 428–434. https://doi.org/10.1016/J. CEJ.2017.04.043.

Li, L., 1998. Improvement of Primary Wastewater Treatment by Sludge Recycling. The Hong Kong University of Science and Technology, Clear Water Bay, Kowloon, Hong Kong. https://doi.org/10.14711/THESIS-B583777.

Mamais, D., Jenkins, D., Prrr, P., 1993. A rapid physical-chemical method for the determination of readily biodegradable soluble COD in municipal wastewater. Water Res. 27, 195–197. https://doi.org/10.1016/0043-1354(93)90211-Y.

Mccarty, P.L., Bae, J., Kim, J., 2011. Domestic wastewater treatment as a net energy producer À can this be achieved? Environ. Sci. Technol 45, 10. https://doi.org/ 10.1021/es2014264.

Meerburg, F., 2016. High-rate Activated Sludge Systems to Maximize Recovery of Energy from Wastewater : Microbial Ecology and Novel Operational Strategies. Gent University.

Miller, M.W., 2015. Optimizing High-Rate Activated Sludge: Organic Substrate for Biological Nitrogen Removal and Energy Recovery. PhDThesis. Faculty of the Virginia Polytechnic Institute and State University, Blacksburg.

Miller, M.W., Elliott, M., DeArmond, J., Kinyua, M., Wett, B., Murthy, S., Bott, C.B., 2017. Controlling the COD removal of an A-stage pilot study with instrumentation and automatic process control. Water Sci. Technol. 75, 2669–2679. https://doi.org/ 10.2166/wst.2017.153.

Miller, M.W., Jimenez, J., Murthy, S., Kinnear, D., Wett, B., Bott, C.B., 2013. Mechanisms of COD removal in the adsorption stage of the A/B process. In: 86th Annual Water Environment Federation Technical Exhibition and Conference, WEFTEC 2013. Water Environment Federation, pp. 2472–2481. https://doi.org/10.2175/ 193864713813673721.

Modin, O., Persson, F., Wilén, B.-.M., Hermansson, M., 2016. Nonoxidative removal of organics in the activated sludge process. 10.1080/10643389.2016.1149903 46, 635–672. https://doi.org/10.1080/10643389.2016.1149903.

Nogaj, T., 2015. Mathematical Modeling of Carbon Removal in the A-Stage Activated Sludge System.

Nogaj, T., Randall, A., Jimenez, J., Takacs, I., Bott, C., Miller, M., Murthy, S., Wett, B., 2015. Modeling of organic substrate transformation in the high-rate activated sludge process. Water Sci. Technol. 71, 971–979. https://doi.org/10.2166/wst.2015.051.

Rahman, A., De Clippeleir, H., Thomas, W., Jimenez, J.A., Wett, B., Al-Omari, A., Murthy, S., Riffat, R., Bott, C., 2019. A-stage and high-rate contact-stabilization performance comparison for carbon and nutrient redirection from high-strength municipal wastewater. Chem. Eng. J. 357, 737–749. https://doi.org/10.1016/J. CEJ.2018.09.206.

Rahman, A., Meerburg, F., Ravadagundhi, S., Wett, B., Jimenez, J., Bott, C., Al-Omari, A., Riffat, R., Murthy, S., De Clippeleir, H., 2016. Bioflocculation management through high-rate contact-stabilization: a promising technology to recover organic carbon from low-strength wastewater. Water Res. 104, 485–496. https://doi.org/10.1016/j. watres.2016.08.047.

Rahman, A., Mosquera, M., Thomas, W., Jimenez, J.A., Bott, C., Wett, B., Al-Omari, A., Murthy, S., Riffat, R., De Clippeleir, H., 2017. Impact of aerobic famine and feast condition on extracellular polymeric substance production in high-rate contact stabilization systems. Chem. Eng. J. 328, 74–86. https://doi.org/10.1016/J. CEJ.2017.07.029.

Regmi, P., Miller, M.W., Holgate, B., Bunce, R., Park, H., Chandran, K., Wett, B., Murthy, S., Bott, C.B., 2014. Control of aeration, aerobic SRT and COD input for mainstream nitritation/denitrition. Water Res. 57, 162–171. https://doi.org/ 10.1016/J.WATRES.2014.03.035.

Rey-Martínez, N., Barreiro-López, A., Guisasola, A., Baeza, J.A., 2021. Comparing continuous and batch operation for high-rate treatment of urban wastewater. Biomass Bioenergy 149, 106077. https://doi.org/10.1016/j.biombioe.2021.106077.

Ross, R.D., Crawford, G.V., 1985. Influence of waste activated sludge on primary clarifier operation. J. Water Pollut. Control Fed. 57, 1022–1026.

Rosso, D., 2019. Carbon capture and management strategies for energy harvest from wastewater | the Water Research Foundation.

Sancho, I., Lopez-Palau, S., Arespacochaga, N., Cortina, J.L., 2019. New concepts on carbon redirection in wastewater treatment plants: a review. Sci. Total Environ. 647, 1373–1384. https://doi.org/10.1016/J.SCITOTENV.2018.08.070.

Seeley, I.H., 1992. Wastewater engineering. Public Works Engineering. McGraw-Hill, New York, pp. 160–214. https://doi.org/10.1007/978-1-349-06927-9_4.

Taboada-Santos, A., Rivadulla, E., Paredes, L., Carballa, M., Romalde, J., Lema, J.M., 2020. Comprehensive comparison of chemically enhanced primary treatment and high-rate activated sludge in novel wastewater treatment plant configurations. Water Res. 169, 115258 https://doi.org/10.1016/j.watres.2019.115258.

Takács, I., 2021. SUMO user manual [WWW Document].

Tirkey, V., Goonesekera, E.M., Kovalovszki, A., Smets, B.F., Dechesne, A., Valverde-Pérez, B., 2022. Short sludge age denitrification as alternative process for energy and nutrient recovery. Bioresour. Technol. 366, 128184 https://doi.org/10.1016/j. biortech.2022.128184.

Van Winckel, T., Liu, X., Vlaeminck, S.E., Takács, I., Al-Omari, A., Sturm, B., Kjellerup, B. V., Murthy, S.N., De Clippeleir, H., 2019. Overcoming floc formation limitations in high-rate activated sludge systems. Chemosphere 215, 342–352. https://doi.org/ 10.1016/J.CHEMOSPHERE.2018.09.169.

Versprille, A.I., Zuurveen, B., Stein, T., 1985. The A–B process: a novel two stage wastewater treatment system. Water Sci. Technol. 17, 235–246. https://doi.org/ 10.2166/WST.1985.0133.

Wett, B., Aichinger, P., Hell, M., Andersen, M., Wellym, L., Fukuzaki, Y., Cao, Y.S., Tao, G., Jimenez, J., Takacs, I., Bott, C., Murthy, S., 2020. Operational and structural A-stage improvements for high-rate carbon removal. Water Environ. Res. 92, 1983–1989. https://doi.org/10.1002/wer.1354.

Wett, B., Buchauer, K., Fimml, C., 2007. Energy self-sufficiency as a feasible concept for wastewater treatment systems. In: IWA Leading Edge Technology Conference. Singapore, pp. 21–24.

Wilén, B.-.M., Lumley, D., Mattsson, A., Mino, T., 2006. Rain events and their effect on effluent quality studied at a full scale activated sludge treatment plant. Water Sci. Technol. 54, 201–208. https://doi.org/10.2166/WST.2006.721.

Yeshi, C., Leng, L.C., Li, L., Yingjie, L., Seng, L.K., Ghani, Y.A., Long, W.Y., 2014. Mass flow and energy efficiency in a large water reclamation plant in Singapore. J. Water Reuse Desalin. 3, 402–409. https://doi.org/10.2166/WRD.2013.012.

Yetis, Tarlan, E., 2002. Improvement of primary settling performance with activated sludge. Environ. Technol. (United Kingdom) 23, 363–372. https://doi.org/10.1080/ 09593332508618395.

Zhang, C., Guisasola, A., Baeza, J.A., 2021. Achieving simultaneous biological COD and phosphorus removal in a continuous anaerobic/aerobic A-stage system. Water Res. 190, 116703 https://doi.org/10.1016/j.watres.2020.116703.